Experimental Investigation of the Distribution of Two-Phase Flow in Oil-Injected Twin-Screw Compressors

Matthias Heselmann, Ulrich Dämgen, and Andreas Brümmer

Abstract Oil-injected twin-screw compressors are the dominating compressor type in the industry. Compressors differ, depending on the manufacturer, in the rotor profile, the lobe number combination, the rotor diameter ratios, the wrap angle, the oil injection position, the oil injection quantity, etc. Historically, they all were probably mainly designed and optimised by trial and error, e.g. by experimentally varying the oil injection quantity, the injection nozzle and its position, or by modifying the profile. However, for some years now, computational modeling has taken an increasingly large part. Although the efficiency of the compressors is satisfying, there is still a remaining potential for improvements. In order to optimise machines by simulation a detailed knowledge of the loss mechanisms due to oil in the working chambers and approaches for their calculation are required. Therefore, for this work, as a first step for developing these models a series compressors' housing is exchanged with a transparent glass housing in order to visualise the oil during the whole working process. First approaches for calculating the hydraulic losses are proposed and analysed in combination with the measurements.

Keywords Twin-screw compressor · Oil-injection · Oil distribution · Hydraulic loss · Transparent housing

Nomenclature

a	acceleration [m/s^2]
A	area [m^2]
e	specific energy [W/kg]
h	height [m]

M. Heselmann (✉) · A. Brümmer
TU Dortmund University, 44227 Dortmund, Germany
e-mail: matthias.heselmann@tu-dortmund.de
URL: https://ft.mb.tu-dortmund.de/en/

U. Dämgen
BOGE KOMPRESSOREN, Otto Boge GmbH, 33739 Bielefeld, Germany

© The Author(s), under exclusive license to Springer Nature Switzerland AG 2024

M. Read et al. (eds.), *13th International Conference on Compressors and Their Systems*, Springer Proceedings in Energy, https://doi.org/10.1007/978-3-031-42663-6_6

l	length [m]
$\dot{m}$	mass flow rate [kg/s]
n	rotational speed [1/s]
n	polytropic exponent [–]
p	pressure [Pa]
P	power [W]
R	radius [m]
t	time [s]
u	circumferential speed [m/s]
v	velocity [m/s]
v_i	inner volume ratio [–]
$\dot{V}$	volume flow rate [m^3/s]
w	width [m]
W	work [J]
β	angular range [°]
β	lead angle [rad]
$\dot{\gamma}$	shear rates [1/s]
Δ	difference [–]
η	dynamic viscosity [Pas]
ϑ	temperature [°C]
Π	pressure ratio (compressor) [–]
τ	density [kg/m^3]
ρ	shear stress [Pa]
$\dot{\Phi}$	power loss [W]

Subscript

acc	acceleration
c	clearance
e	effective
FR	female rotor
fric	friction
g	gas
hp	high pressure side
imp	impulse
in	injection
kin	kinetic
lp	low pressure side
m	mixture
MR	male rotor
N	standard condition (1013.25 hPa, 273.15 K)
n	normal direction
o	oil

o.f.s.	of full scale
o.r.	of reading
pipe	in pipe behind filter
rel	relativ
spec	related to standard volume flow rate
t	tangential direction
tank	oil tank
tip	rotor tip
u	circumferential direction

1 Introduction

Twin-screw compressors in general consist of two helical rotors enclosed in a tight housing. In wet-running application, an auxiliary fluid (usually oil) is injected into the working chambers. This compressor type dominates the market, used for compression of air, refrigerants, or process gas in industry. The injected fluid increases the efficiency of the compressor type significantly due to sealing the gaps and dissipating the compression heat. The biggest disadvantage are the so-called hydraulic losses, caused by the oil, which causes additional friction. These losses are responsible for the reduced circumferential speeds of wet-running screw compressors compared to dry-running screw compressors [1–3].

Beside the compressor's geometry itself the amount of injected fluid, circumferential tip speed and the fluid viscosity significantly influence the compressor operation. To consider the influence of injected fluid in calculations Kauder introduced the surge hypothesis, which describes the formation of a liquid surge in front of the rotor teeth [4]. Further research can be divided mainly into two priorities; the loss mechanisms caused by the injected fluid and the distribution of the injected fluid in the working chambers.

To investigate the loss mechanisms, the individual effects on the compressor performance are isolated. According to Deipenwisch, who considers oil as auxiliary fluid, the loss mechanisms are identified as frictional, momentum and acceleration losses [5]. Frictional losses occur due to the viscous shear of the fluid. The momentum loss describes the periodic acceleration of the fluid attached to the walls, by the passing rotor surface. The acceleration loss is the acceleration of the injected fluid to the circumferential tip speed. The influence of injected water into a screw expander has been investigated by Nikolov in terms of indicator diagrams [6]. It shows the same tendencies as injected oil. The latest study chose a more overall approach to describe the hydraulic losses in terms of a torque loss coefficient [7]. The loss coefficient is determined by experiment and depends as well on the circumferential tip speed and the amount of injected fluid.

In order to investigate the fluid distribution it is necessary to observe the fluid behavior within the working chambers. This is a difficult task if the geometry should not be simplified. The investigation of the oil distribution includes the oil injection

itself, e.g. if the injected fluid atomises, the movement of the fluid on the rotor surface and housing bores and the behavior of the fluid in the gaps. These issues were first addressed by Harling, who conducted extensive experimental studies on the distribution of the injected oil in the compressor. He validated his models by means of windows in his compressor housing and found in general good agreement even if he was not able to capture some issues, e.g. bubbles in the liquid surge, or sealing of the housing gap [8]. He described the restrictions of the optical analysis and proposed further investigation with improved optical tools. With increasing computing power it becomes possible to simulate positive displacement machines like the screw machine with computational fluid dynamics. Those simulations show good agreement with experiments in shaft power and mass flow rate of gas [9]. However, the currently available grids for twin screw compressors can not capture the oil film which affects sealing the gaps [10].

As the authors in [5, 10] propose, it is desirable to validate their models with experiments. In this work a test rig is presented containing a series oil-injected screw compressor with a transparent casing. High speed recordings are used to contribute to the validation of the developed models.

2 Experimental Setup

To visualise the oil within the working chambers, a series, direct-drive, oil-injected screw compressor is modified and connected to the experimental test rig outlined in Fig. 1. The modifications mainly concern the space required for high-speed recordings and the installation of measuring equipment. This means electric motor and compressor are elevated to provide more space and the distance between electric motor and compressor is increased to install a torque measuring shaft to record the shaft power. To further explain the test rig, it is divided into the fluid paths air (black), oil (brown) and water (blue). The arrows symbolise the flow direction.

The air is sucked in through an intake filter. At the suction port of the compressor pressure $p_{lp,g}$ and temperature $\vartheta_{lp,g}$ of the gas are measured. At the high pressure side, the pressure $p_{hp,m}$ and temperature $\vartheta_{hp,m}$ are measured where the index m indicates a mixture of air and oil. The mixture is fairly separated in the oil tank and than passes an oil filter, so that the remaining oil is reduced to a minimum. Pressure measurements $p_{tank,g}$ in the oil tank and behind the oil filter $p_{pipe,g}$ gives information of the status of the filter. The delivery mass flow rate is measured with a Coriolis sensor. The valve is used to control the pressure in the system. At last the air is released in the atmosphere through a sound absorber.

For the oil injection circuit no oil pump is needed. The circuit starts in the oil tank and is driven by the pressure difference between the oil tank $p_{tank,g}$ and the injection nozzle at the compressor $p_{in,o}$. In order to control the oil temperature in the tank $\vartheta_{tank,o}$ to about 78°C a thermostat is implemented. For higher temperatures the oil passes a heat exchanger with an additional cooling circuit and for lower temperatures the heat exchanger is bypassed. Pressure $p_{in,o}$ and temperature $\vartheta_{in,o}$ are measured

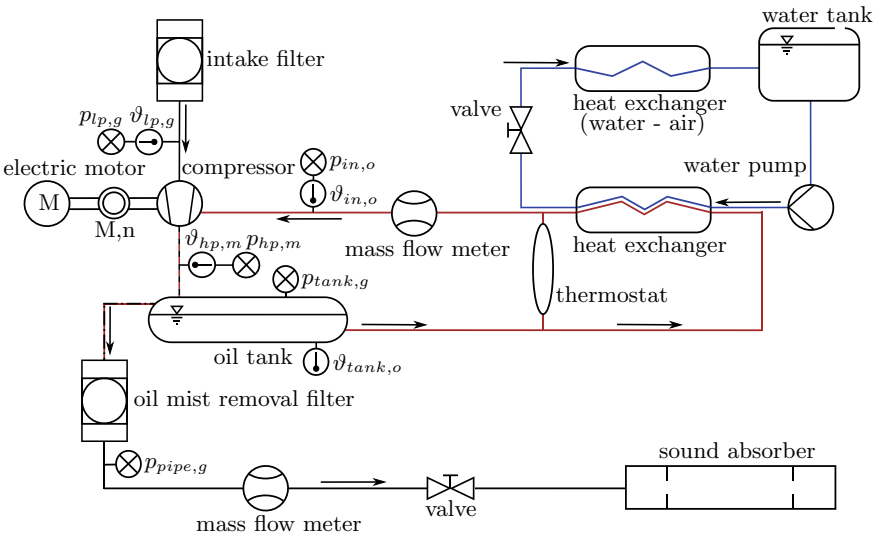

Fig. 1 Schematic representation of the compressor test rig

Table 1 Measuring range and uncertainty of the installed measuring devices

Parameter	Range	Uncertainty	Type (Manufacturer)
p	−1-16 bar(g)	±1 % o.f.s.	Danfoss MBS 3000
ϑ	−185-300 °C	±1 °C (− 40-133 °C)	thermocouples type T
Mass flow rate (oil)	0–6,500 kg h^{-1}	±0.1 % o.r. ($\dot{m}$ > 200 kg h^{-1})	Proline Promass F300 (Endress + Hauser)
Mass flow rate (gas)	0–900 kg h^{-1}	< 0.35 % o.r. ($\dot{m}$ > 643 kg h^{-1})	Proline Promass 83F (Endress + Hauser)
Torque	±200 Nm	±0.05 % o.f.s.	ETH DRVL-III-200-n-1
Rotational speed	max. 13,500 min^{-1}	–	(ETH-messtechnik)

directly before the injection and a Coriolis sensor is implemented to measure the mass flow rate of the oil. The circuit is closed when the gas-oil mixture enters the oil tank again. The water cooling circuit is driven by a centrifugal pump with a water tank, a heat exchanger and valve to control the flow rate.

Detailed information about the range, uncertainty and type of the measuring devices are given in Table 1. The essential measuring device is a high-speed camera for recording the flow pattern of the oil within the working chambers of the screw compressor. The experimental procedure is designed for steady-state conditions in terms of pressure ratio, rotational speed and temperatures.

Table 2 Geometric data of the compressor

Designation	Male rotor (MR)	Female rotor (FR)
Number of lobes	5	6
Rotor lead	253.2 mm	303.84 mm
Rotor profile	Developed by BOGE	
Built-in volume ratio	4.3	
Shaft center distance to male rotor diameter ratio	0.72	
Length to male rotor diameter ratio	1.66	
Female to male rotor diameter ratio	0.8	
Clearance heights	0.04-0.08 mm	

2.1 Operation Point and Compressor

The baseline compressor package BS-62 SLF is provided by BOGE KOMPRESSOREN Otto Boge GmbH & Co. KG. It is a direct-drive compressor stage with a nominal power of 55 kW. For the investigations planned, the electric motor is bigger than the series application motor to ensure operation even at operating points far outside the series application. The outlet is designed for discharge pressures from 9 to 10 bar(a). The profile is carefully designed with respect to a small blowhole on the high pressure side. The lobe combination is 5 + 6 and the ratio of rotor length to rotor diameter is designed for relatively big outlet opening and low deflection of the rotors under pressure [11]. Table 2 summarises some key ratios of the compressor. As already mentioned the series housing is exchanged with a glass housing. This is shown in Fig. 2 with the depicted high pressure side of the compressor. On the left hand side the stage is shown direct after assembling. The right hand side shows a flash light photo during operation at driving speed of 50 Hz, respectively 20 m s^{-1} circumferential speed of male rotor at a compression end pressure of 7 bar(a).

2.2 Reference Measurements

In this section the compressor with the glass housing is compared to the series compressor. Therefore the pressure ratio is kept constant at a pressure ratio $\Pi \approx 7$, which is low compared to the designed inner volume ratio. Figure 3 shows the shaft power P_e, the standard volume flow rate $\dot{V}_N$ and the specific power P_{spec} as a function of the rotational speed n. The standard volume flow rate as well as the shaft power of the series machine increases nearly linearly with increasing rotational speed. While the volume flow rate of the compressor with the glass housing is slightly below the

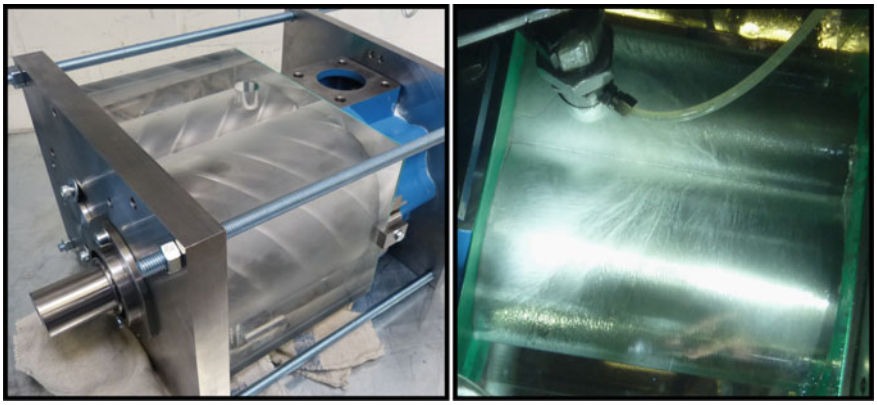

Fig. 2 Photographs of the glass compressor after assembling and during operation at 20 m s^{-1} at compression end pressure of 7 bar(a)

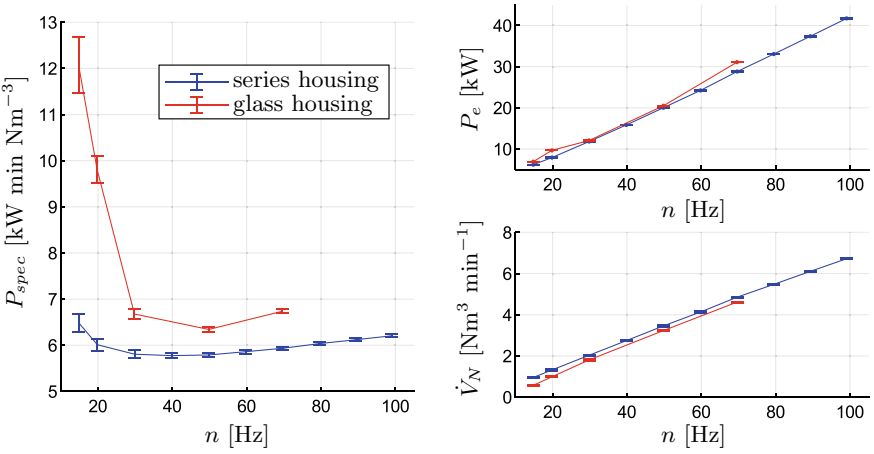

Fig. 3 Measurements and uncertainties comparing series and glass compressor

series compressor, its shaft power is slightly higher. This leads to a large deviation of the specific power for low rotational speeds that decreases for higher rotational speeds. The main part responsible for the uncertainties is the mass flow measurement, since the mass flow rate for rotational speeds of 15 and 20 Hz is at the lower range of the sensor. Furthermore, it should be mentioned that there were some manufacturing issues with the glass housing. This means that the housing bores are slightly larger than that of the series housing (approx. 0.24-0.26 mm). Therefore, the profile had to be modified (crown and root circle) with the given axis distance as boundary condition. It should be noted, that the standard volume flow rate of the compressor with the glass housing is nevertheless smaller than that of the series compressor. This could indicate a changed gap situation either due to the addressed changed profile or

due to a mis-location of the housing to the rotors. The mis-location would change the gap situation in such a way, that the housing gap in particular would become smaller on the probably less important low-pressure side and larger on the high-pressure side.

3 Modeling Hydraulic Losses

The need to model hydraulic losses results from the chosen simulation itself. If the simulation covers e.g. all containing fluids (gas and oil) with all their properties (film formation, momentum exchange, inhomogeneous distribution, etc.), the compressor stage can be calculated without extra models. This is the case when multiphase flow simulations are performed with computational fluid dynamics [9, 10]. However, the requirements for the mesh used are high and the solution of the system of equations computationally intense. As a result, this method is more suitable for detailed recalculation and for visualization purposes than for performing numerous geometric variations. For these purposes, the chamber model simulation is suitable. Basic equations here are only the conservation of mass and energy. The drawback is that several assumptions have to be made and submodels have to be developed. An overview of some submodels containing models for the mass flow rate and heat transfer is given in [12].

However, the complex calculation of non-miscible multiphase content in one chamber e.g. oil and air, is not yet fully implemented. The calculation of oil-injected compressors requires three further steps compared to dry running compressors.

1. The mass flow rates through all connections (front gaps, housing gaps, inter-lobe clearance, blowhole, suction and discharge port) must take into account two-phase flow models. This takes into account the sealing of the gaps by the auxiliary fluid.
2. Some model has to be chosen to take into account the heat dissipated by the oil.
3. A model that accounts for hydraulic losses must be used to account for the adverse effects of oil injection.

In the following, the experiments with the compressor with the glass housing, the high-speed recordings are used to investigate the influence of the individual loss mechanisms. The loss models are taken from [5].

3.1 Acceleration Power Loss

According to Deipenwisch, one part of the hydraulic power loss occurs immediately after injection, because the majority of the oil is injected in the radial direction. Smaller portions of the oil enter the working chambers elsewhere, e.g. oil disposal holes of the bearing seats. To estimate this power loss $\dot{\Phi}_{acc}$ it is assumed that:

- The injected oil has no circumferential velocity ($v_{rel} = 0$).
- The whole amount of injected oil is accelerated to circumferential tip speed ($v_{rel} = u_{tip}$).
- The sucked in air needs to be accelerated, too (entire mass flow is considered).
- The mass flow is equally distributed between male and female chambers.

Using the specific kinetic energy e_{kin} and the entire mass flow rate $\dot{m}_m$ the power loss due to acceleration $\dot{\Phi}_{acc}$ can be expressed as:

$$\dot{\Phi}_{acc} = \dot{m}_m \cdot e_{kin} = \frac{1}{4} \cdot \dot{m}_m \cdot u_{MR}^2 + \frac{1}{4} \cdot \dot{m}_m \cdot u_{FR}^2 \tag{1}$$

The circumferential tip speed of the rotors is represented by u_{MR} of the male rotor and u_{FR} of the female rotor, respectively. This approach presents an upper estimation of the power loss, since the entire mass must be accelerated to tip speed. Therefore, the rotors are not wetted by the oil e.g. in the root circle area [5].

For the used glass housing oil injection takes place in the radial direction at the female rotor side near the discharge port. High speed recordings are done and analysed. Figure 4 visualises some impressions from the high pressure side at rotational speed of 50 Hz. The oil is represented by the white/foamy areas in the photographs due to the reflection of the light. Areas, where the oil builds a film at the housing are transparent. Each photo is supported by an image showing the main flow directions of the oil in the form of sketched arrows. As the rotor tip is visible, this indicates that the housing gaps of both rotors are well sealed. After passing the housing gap, the oil flow is decelerated and a border line between foamy and transparent areas is formed that slightly varies with the rotation angle. This border is represented by the black line. The red dashed line represents the border of the first image and thus, in comparison to the black line, the movement of the decelerated oil border. At the male rotor the border is approximately at a constant distance behind the rotor tip. This is not identified at the female rotor. It is observed, that the injected oil influences the oil film for more than one tooth gap, as the female rotor tip passes the injection port.

3.2 Fluid Friction Power Loss

Fluid friction is considered in the narrow clearances with regard to the oil, due to the significant higher viscosity compared to air. Therefore, it is assumed that:

- The clearance is completely filled with oil.
- Couette-flow is considered.
- Shear stresses τ are superposed with a pressure gradient Δp.
- The cross section relevant for the friction is formed by the width of the clearance w_c and effective length of the clearance l_c ($A_c = w_c \cdot l_c$).
- The shear rates $\dot{\gamma}$ are calculated from the relative velocity v_{rel} of the boundary and the minimum gap height h_c ($\dot{\gamma} = v_{rel} / h_c$).

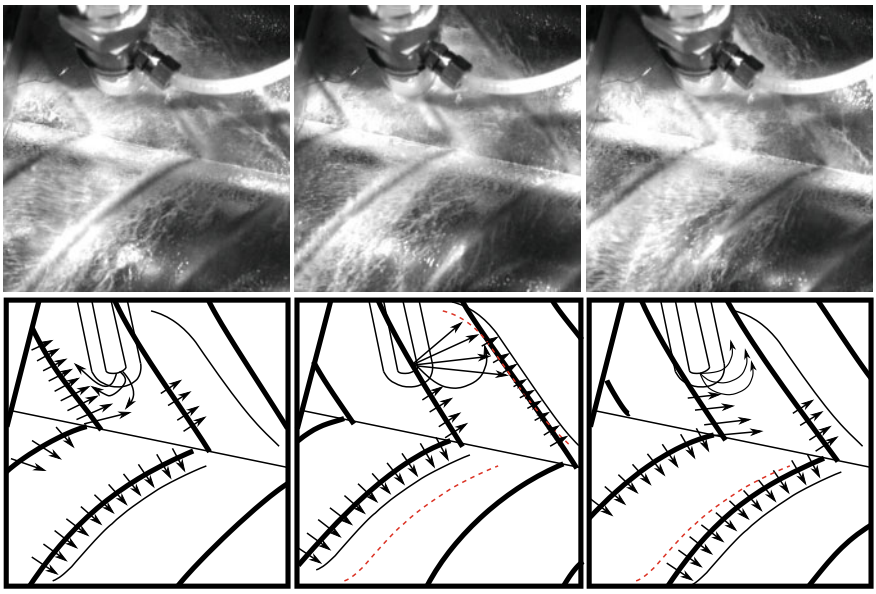

Fig. 4 Images from the high pressure side of the compressor (at oil injection) for a tip speed of $u_{MR} \approx 20\,\mathrm{m\,s^{-1}}$ and oil mass flow rate of $\dot{m}_o \approx 23\,\mathrm{kg\,min^{-1}}$

The effective length l_c of the gap represents not only the area with minimum gap height, but also the area in front of the rotor tooth where an oil surge is formed. This forms, when the sum of the oil from the oil film on the housing surface in front of the gap and the oil flowing into the gap from the leading tooth flank is greater than the amount of oil that can flow out again through the housing gap [5]. The power loss due to fluid friction $\dot{\Phi}_{fric}$ can be calculated as:

$$\dot{\Phi}_{fric} = A_c \cdot \tau \cdot v_{rel} = \frac{w_c \cdot l_c \cdot \eta \cdot u^2}{h_c} + \frac{\Delta p \cdot h_c \cdot w_c \cdot u}{2} \tag{2}$$

The dynamic viscosity of the oil is represented by η. The relative velocity v_{rel} corresponds to the circumferential speed of the considered clearance (housing gap or front gap). The identification of $l_c = \frac{\beta \cdot \pi}{180^\circ} \cdot R_{tip}$, where R_{tip} is the crown circle radius of the considered rotor, is described by Harling according to a lubrication gap flow. It is assumed, that a liquid surge forms in an angular range of $\beta = 15^\circ$ in front of the male rotor, without violating the underlying model. It is mentioned that this angle is more valid for the male rotor than for the female rotor, because of the small curvatures of the female rotor contour [8]. More recent are experimental investigations of Vasuthevan. Herein, different profile contours are turning in a cylindrical housing, which is filled with a specified amount of liquid. The angle range is determined to $\beta = 30^\circ$ for a rectangular profile. However, the experiments have been done at atmospheric pressure conditions (without pressure gradient) [7].

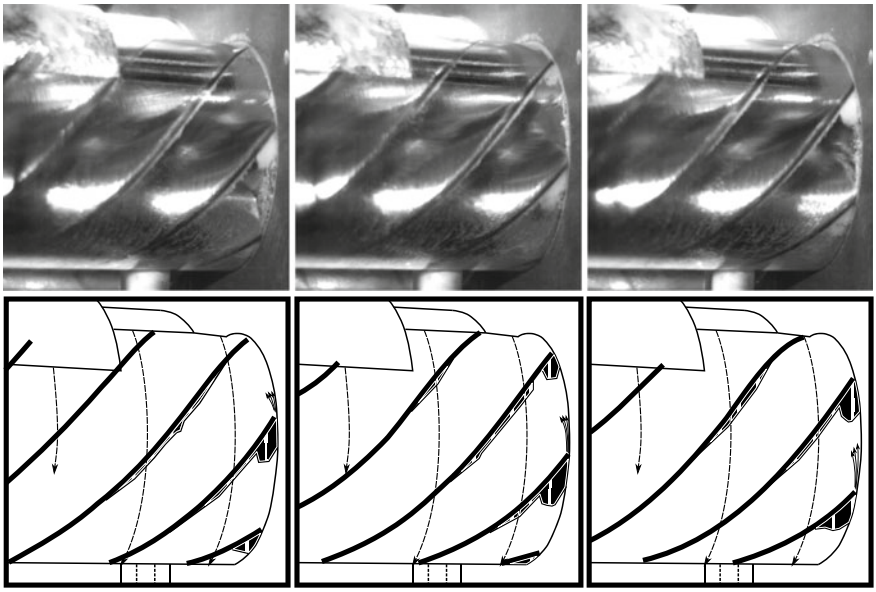

Fig. 5 Impressions from the female rotor side of the compressor for a male rotor tip speed of $u_{MR} \approx 20\,\mathrm{m\,s^{-1}}$ and oil mass flow rate of $\dot{m}_o \approx 23\,\mathrm{kg\,min^{-1}}$

The calculation of the power loss due to friction is therefore dependent on the gap width and length as geometric parameters. To take a closer look at the assumptions made, Fig. 5 shows images of the female rotor at male rotor driving speed of 50 Hz. The first image on the left hand side depicts the chamber closure from the suction port. The foamy oil at the surface of the suction port indicates that oil distributes through the whole machine. Centrifugal forces throw the oil into the suction port, where it forms a film on the wall and runs back towards the chamber until it is collected by the female rotor tooth again; the same is observed for the male rotor which is not shown. From this point, there is an oil surge forming in front of the rotor tip sketched in the images below the photographs on Fig. 5. This oil surge in general moves normal to the rotor tooth. Due to the lead of the rotor, the circumferential acceleration can be decomposed in a normal and tangential component, shown in Fig. 6. Therefore the amount of oil within the oil surge increases towards the high pressure side. This decomposition depends on the lead of the rotor, the lead angle β respectively. The transport in the axial direction therefore increases when the rotor lead decreases, respectively the wrap angle increases if the rotor length is constant. When it reaches the front end of the housing it is strongly redirected in an almost pure circumferential direction. Observing this oil accumulation, a flow is detected where it is not clear whether it flows through the housing gap or the front gap. However, this flow does not start directly, but only with further rotation and an associated increase in pressure difference over the gap.

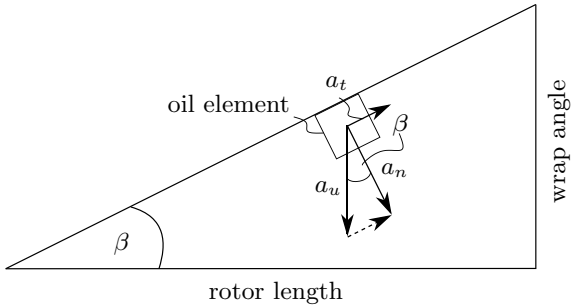

Fig. 6 Accelerations acting on an oil element in front of the rotor on unwound rotor

As before, there is nearly no air flow through the housing gap visible. Thus it can be deduced, that the housing gap is completely filled with oil as no spray or foamy parts are observed. A further clue is given by the circumferential smear sketched by the dashed lines.

3.3 Momentum Power Loss

The oil films on the housing and the rotors get periodically accelerated by the passing rotor tooth and rotor flanks, respectively. This causes an impulse power loss $\dot{\Phi}_{mom}$. Assumptions to express this loss by an equation are:

- The gap is completely filled with oil.
- A linear flow profile forms until the end of the gaps.
- The entrance velocity of the oil in the gap is negligible.
- The gap flow is comparable with a plane wall that is suddenly moved.

Thus, the momentum power loss $\dot{\Phi}_{mom}$ can be determined by:

$$\dot{\Phi}_{mom} = \frac{dW_{acc}}{dt} = \frac{1}{6} \cdot \frac{u^2 \cdot \rho_o \cdot h_c \cdot w_c \cdot l_c}{\frac{l_c}{u}} \tag{3}$$

For the housing gap, the relative velocity equals the circumferential tip speed of the rotor $u = u_{MR}$ for the male rotor and $u = u_{FR}$ for the female rotor, respectively. For the front gap, the circumferential speed increases with the radius of the gap segment considered ($u = u(r)$) [5].

As already pointed out, there must be a film of oil on the housing bore surfaces, as the rotor tips are clearly visible. Therefore Fig. 7 focuses on the pockets between two rotor tips, of the male rotor at circumferential speed of $u_{MR} = 20\,\mathrm{m\,s^{-1}}$. The black rectangle is a bracket against mis-location of the housing. The black and gray stained area is a glass chipping from the housing. For the interpretation of these impressions, the images are divided into two areas. The first in the suction area or at the start of compression (on the right hand side in each case).

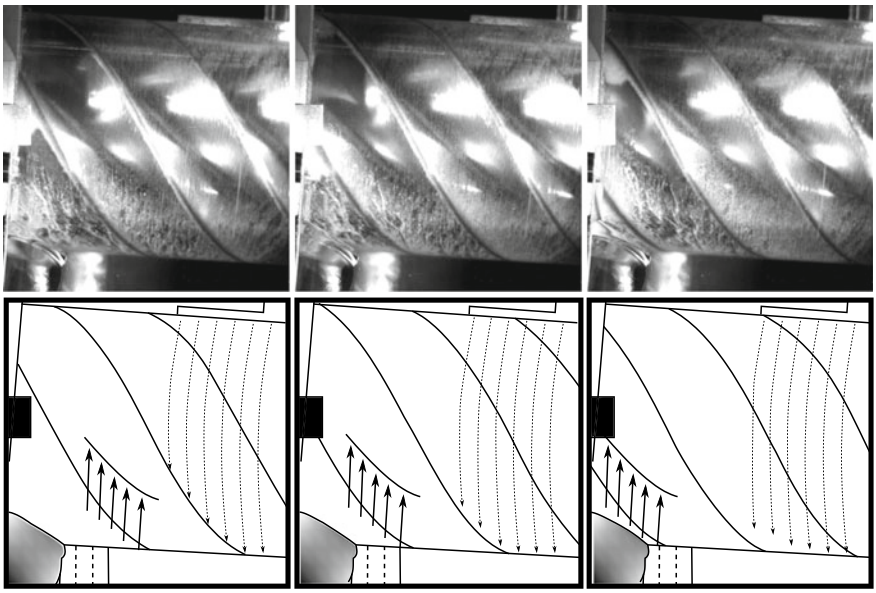

Fig. 7 Impressions from the male rotor side of the compressor for a male rotor tip speed of $u_{MR} \approx 20\,\mathrm{m\,s^{-1}}$ and oil mass flow rate of $\dot{m}_o \approx 23\,\mathrm{kg\,min^{-1}}$

In this area there is nearly no oil surge or pressure gradient. The dashed lines in the sketches accompanying the photos illustrate a slight oil smear in the corresponding area caused by the contact of the rotor tips with the oil film at the housing. This in turn causes a momentum power loss discussed in this section. Analysing the assumptions made, the assumption that a linear flow profile is formed up to the end of the gap is doubtful, since the considered male rotor housing gap has almost no length, especially when there is no oil surge. However, the assumption made represents an upper estimation of the loss in this section. The further the rotor rotation progresses, an oil surge forms and the pressure gradient along the gap increases. As illustrated by the arrows on the left hand side of each the flow through the housing gap becomes foamy, which means that there are some air inclusions or oil spray within the gap. Therefore, the gap cannot be completely filled with oil. Vasuthevan has already shown that the presence of a surge alone excludes a complete sealing of a gap against air, but for water [13]. The pictures shown here underline this also for an oil surge. However, the surge increases the effective length of the gap, so that the assumption of a linear flow profile at the gap outlet becomes more plausible. The line shown marks the area where the oil flow calms down again, i.e. becomes transparent again. This is approximately in the middle between the rotor teeth and it can therefore be assumed that the flow velocity in the oil film is small compared to the velocity in the gap.

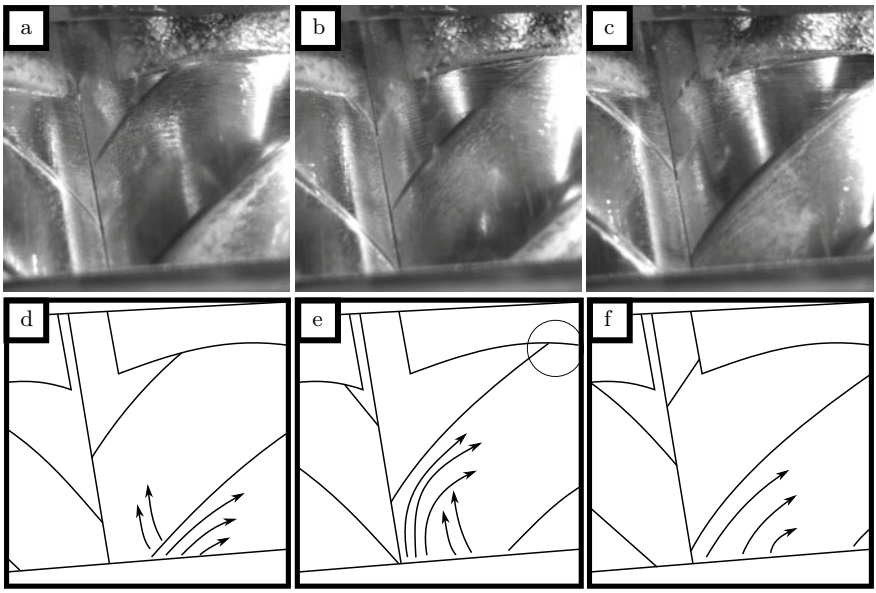

Fig. 8 Impressions from the suction side of the compressor for a male rotor tip speed of $u_{MR} \approx 20\,\mathrm{m\,s^{-1}}$ and oil mass flow rate of $\dot{m}_o \approx 23\,\mathrm{kg\,min^{-1}}$

3.4 Squeezed Oil

One of the main objectives of oil injection is to lubricate the rotors to allow them to roll. Since the rolling takes place in the area of the inter-lobe clearance, it is obvious that there must be oil between the rotors. Taking a closer look to the inter-lobe clearance from the low pressure side towards the high pressure side, there are two main issues which might cause some serious power losses (see Fig. 8). The first issue is based on the large pressure gradient along the inter-lobe clearance due to the fact that at some point a connection from the machine's high pressure side to the low pressure side is established. The circle in Fig. 8e shows, that there is still connection to the suction port, when a lot of oil enters the chamber through the inter-lobe clearance. The second issue is not that obvious considering just the pictures or videos showing the suction side of the compressor. But remembering the injection area (Fig. 4) directly below the area seen here, the amount of oil in the vanishing chambers seems huge. By design, there is a connection from the vanishing chambers to the high-pressure port, but it is conceivable that there is too much oil in the chambers. The forced flow through the moving rotors would then cause a massive increase in pressure. The fluid would be squeezed through the existing connections (gaps and discharge port) and could increase the power consumption significantly. So there are two effects which could be responsible for the sketched flow through the inter-lobe clearance. It is observed that the flow appears suddenly. Considering the

compression process of a screw compressor, a steady flow can be expected through the inter-lobe clearance, except when the compressor is operated outside its design point. In that case, under or over compression occurs. The suddenly appearing flow requires an under compression, because otherwise the fluid would expand in the discharge port. Considering the inner volume ratio of $v_i \approx 4.3$ and a pressure ratio of $\Pi \approx 7$ an under compression could be likely using a polytropic exponent in the range $n \in [1.1;\ 1.3]$. However, there are vanishing chambers anyway which cause a relatively large increase in pressure at the end of the working cycle, especially when there is some oil left in the chamber. This issue could be modified either by changing the outlet or by changing the direction of injection. The latter will be investigated in the future.

4 Conclusion

In this paper, hydraulic losses in a twin-screw compressor with a glass housing are investigated. For this purpose, the cast housing of a commercial machine is replaced by a glass housing so that insights into the entire machine can be achieved. High-speed recordings of the compressor in operation are made and the plausibility of the assumptions of the existing loss models is examined and an oil film is detected on the entire housing. An oil surge is formed almost immediately at the start of compression. The oil is mainly transported through the machine normal to the rotor tooth. Particularly in the area near the discharge port, large quantities of oil occur, some of which is squeezed through the inter-lobe clearance into working chambers that are still in connection with the suction port. So far the operation point was set to a relative small pressure ratio of $\Pi \approx 7$ to avoid a break down of the glass housing. In future works it is planned to set the operation point to the design point of the compressor. Different injection nozzles will be analysed with respect to the oil distribution within the compressor. The overall aim is to generate a model which accounts for the oil distribution within a machine.

References

1. L. Rinder, *Schraubenverdichter* (Springer-Verlag, Wien New York, 1979)
2. H. Kauder, Das Öl im Schraubenkompressor - Ein Faktor für optimale Betriebsverhältnisse. Pumpen Vakuumpumpen Kompressoren ’87 71075, pp, 38–44 (1987)
3. J.S. Fleming, C.X. You, Y. Tang, *Rotor Tip Design in Oil Injected Helical Twin Screw Compressors With Respect to Viscous Friction Loss* (Institution of Mechanical Engineers Conference Publications, Medical Engineering Publications Ltd., 1994), pp. 115–121
4. K. Kauder, Energiewandlung in öleingespritzten Schraubenverdichtern. Technische Mitteilungen **72**(6), 404–10 (1979)
5. R. Deipenwisch, Ein Beitrag zum Einsatz von Öl als Konstruktionselement in Schraubenmaschinen. Dissertation University Dortmund (2000)

6. A. Nikolov, A. Brümmer, Analysis of indicator diagrams of a water injected twin-shaft screw-type expander, in *International Compressor Engineering Conference*. Paper 2492 (2016). https://docs.lib.purdue.edu/icec/2492/
7. H. Vasuthevan, A. Brümmer, Generic experimental investigation of hydraulic losses within twin-screw machines, in *The 9th International Conference on Compressor and Refrigeration* (2019)
8. H.B. Harling, Untersuchung zur Ölverteilung in Schraubenkompressoren mit Schmiermitteleinspritzung. Dissertation University Dortmund (1993)
9. S.R. Rane, A. Kovacevic, N. Stosic, CFD Analysis of oil flooded twin screw compressors, in *International Compressor Engineering Conference*. Paper 2392 (2016). https://docs.lib.purdue.edu/icec/2392
10. N. Basha, *Numerical Analysis of Oil Injection in Twin-screw Compressors*. Ph.D. thesis City, University of London (2021). https://openaccess.city.ac.uk/id/eprint/26572/
11. BOGE KOMPRESSOREN Otto Boge GmbH & Co. KG, Brochure BOGE airend (2012). https://www.boge.com/sites/default/files/360_en-bi_201212_effilence.pdf
12. M.M. Tanveer, C.R. Bradshaw, X. Ding, D. Ziviani, Mechanistic chamber models: a review of geometry, mass flow, valve, and heat transfer sub-models. Int. J. Refrigeration **142**, 111–126 (2022). https://doi.org/10.1016/j.ijrefrig.2022.06.016
13. H. Vasuthevan, A. Brümmer, Multiphase-flow simulation of a rotating rectangular profile within a cylinder in terms of hydraulic loss mechanisms. IOP Conf. Ser. Mater. Sci. Eng. **425**, 012002. https://doi.org/10.1088/1757-899X/425/1/012002 (2019)